

Electronic Supplementary Information (ESI) for

Facet-Dependent Activity of Hematite Nanocrystals toward Oxygen Evolution Reaction

Toshihiro Takashima,^{*a,b,c} Shota Hemmi,^b Qingyu Liu^c and Hiroshi Irie^{a,b,c}

^a Clean Energy Research Center, University of Yamanashi, 4-3-11 Takeda, Kofu, Yamanashi 400-8511, Japan

^b Integrated Graduate School of Medicine, Engineering and Agricultural Sciences, University of Yamanashi, 4-3-11 Takeda, Kofu, Yamanashi 400-8511, Japan

^c Department of Applied Chemistry, Faculty of Engineering, University of Yamanashi, 4-3-11 Takeda, Kofu, Yamanashi 400-8511, Japan

Contents

ESI-1) HRTEM images of α -Fe₂O₃ nanocrystals. (Figs. S1–3).

ESI-2) Polarization curves at pH 13 normalized by ECSAs. (Fig. S4).

ESI-3) Tafel plots of α -Fe₂O₃ nanocrystals. (Fig. S5).

ESI-4) Polarization curves at pH 7 normalized by ECSAs. (Fig. S6).

ESI-5) Results of kinetic isotope effect experiments. (Fig. S7).

ESI-1) HRTEM images of α -Fe₂O₃ nanocrystals. (Fig. S1).

α -Fe₂O₃ cube

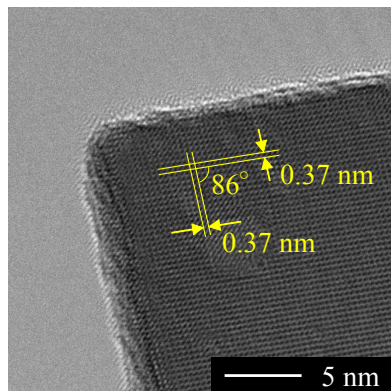


Fig. S1 High-resolution TEM (HRTEM) image of α -Fe₂O₃ cube.

The HRTEM image of α -Fe₂O₃ cube shows an interlaced two-dimension lattice fringes with a dihedral angle of 86° and an interplanar spacing of 0.37 nm, corresponding to the (012) and (10-2) lattice planes, respectively [1,2]. Because both planes belong to the (012) plane class, the α -Fe₂O₃ cube was revealed to be enclosed by the (012) facet.

α -Fe₂O₃ bipyramid

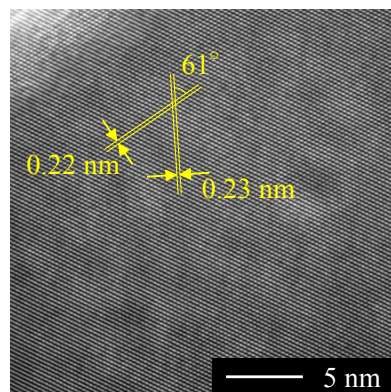


Fig. S2 High-resolution TEM (HRTEM) image of α -Fe₂O₃ bipyramid.

From the HRTEM image of α -Fe₂O₃ bipyramid, the lattice fringes with spacings of 0.22 and 0.23 nm and a dihedral angle of 61° were observed. These are assigned to the (113) and (006) planes,

respectively, and matches well with the ideal geometrical model of α -Fe₂O₃ hexagonal bipyramid enclosed by the (113) facets [3,4].

α -Fe₂O₃ plate

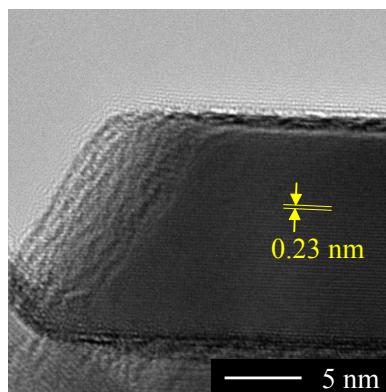


Fig. S3 High-resolution TEM (HRTEM) image of α -Fe₂O₃ plate.

The above HRTEM image is the side view of α -Fe₂O₃ plate. A spacing of the lattice parallel to the top surface was found to be 0.23 nm, corresponding to the distance between the (006) planes [5]. Therefore, the exposed basal plane can be indexed to the (001) facet.

ESI-2) Polarization curves at pH 13 normalized by ECSAs. (Fig. S4).

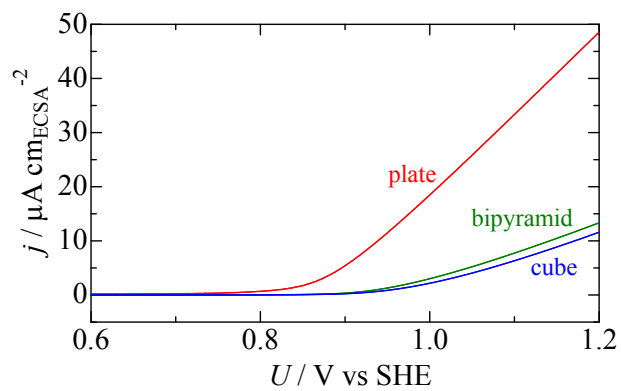


Fig. S4 ECSA-normalized polarization curves of $\alpha\text{-Fe}_2\text{O}_3$ nanocrystals measured at pH 13.

ESI-3) Tafel plots of α -Fe₂O₃ nanocrystals. (Fig. S5).

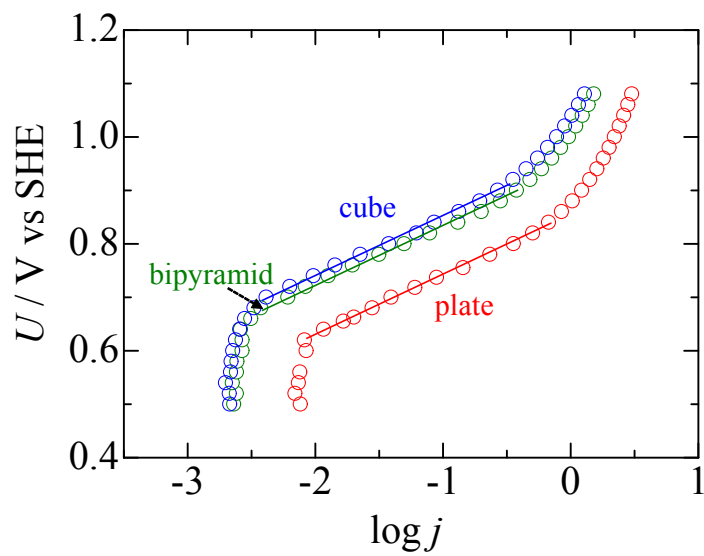


Fig. S5 Tafel plots of α -Fe₂O₃ cube, bipyramid and plate.

ESI-4) Polarization curves at pH 7 normalized by ECSAs. (Fig. S6).

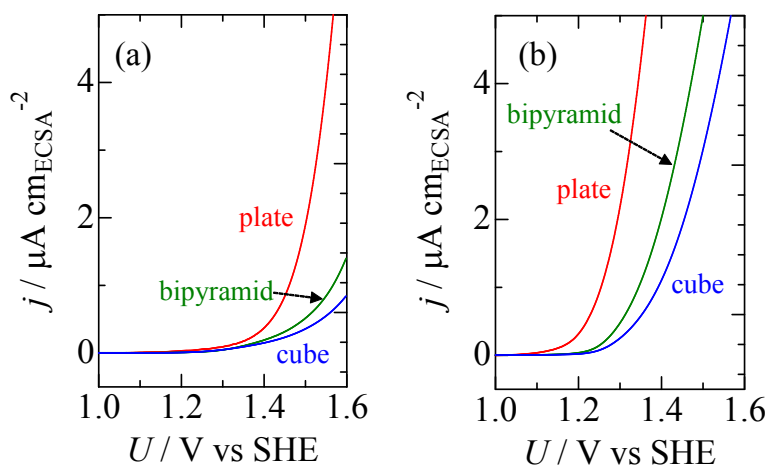


Fig. S6 ECSA-normalized polarization curves of α -Fe₂O₃ nanocrystals measured at pH 7. The measurements were conducted in (a) 0.5 M Na₂SO₄ and (b) the mixture of 0.5 M Na₂SO₄ and 0.05 M lutidine.

ESI-5) Results of kinetic isotope effect experiments. (Fig. S7).

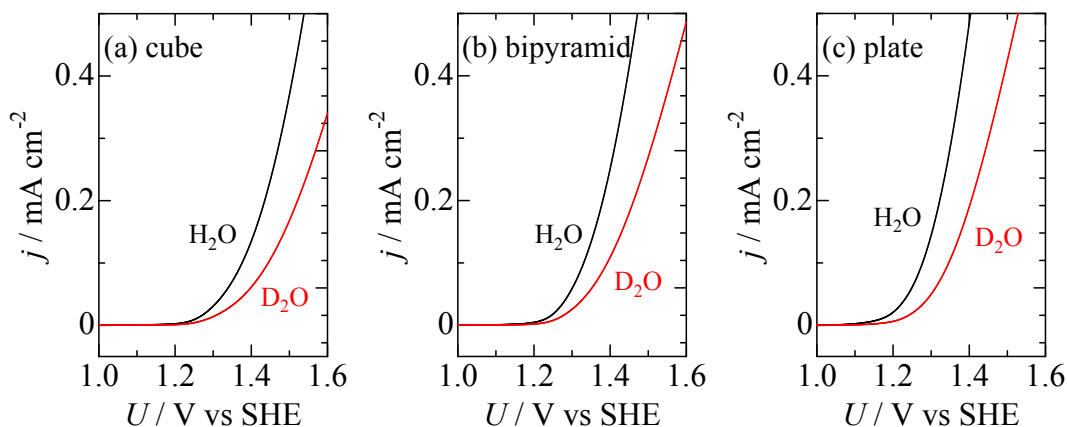


Fig. S7 Polarization curves of $\alpha\text{-Fe}_2\text{O}_3$ with different morphologies ((a) cube, (b) bipyramid and (c) plate) measured to examine the kinetic isotope effect (black line: H_2O , red line: D_2O).

The measurements were conducted at pH (pD) 7 in the presence of lutidine.

When the electrolyte prepared using D_2O instead of H_2O was used, decreases in current density were observed for all the samples, indicating that the kinetic isotope effect appeared. Because the kinetic isotope effect is observed when concerted PCET proceeds, these results indicate that concerted PCET was induced on the surfaces of $\alpha\text{-Fe}_2\text{O}_3$ cube, bipyramid and plate in the presence of lutidine.

References

- [1] C. Wang, C. Zhu, X. Ren, J. Shi, L. Wang and B. Lv, *CrystEngComm*, 2019, **21**, 6390–6395.
- [2] H. Wan, T. Liu, X. Liu, J. Pan, N. Zhang, R. Ma, S. Liang, H. Wang and G. Qiu, *RSC Adv.*, 2016, **6**, 66879–66883.
- [3] M. Lin, L. Tng, T. Lim, M. Choo, J. Zhang, H. R. Tan and S. Bai, *J. Phys. Chem. C*, 2014, **118**, 10903–10910.
- [4] M. Chen, H. Yin, X. Li, Y. Qiu, G. Cao, J. Wang, X. Yang and P. Wang, *J. Hazard. Mater.*, 2020, **395**, 122628.
- [5] M. Zong, X. Zhang, Y. Wang, X. Huang, J. Zhou, Z. Wang, J. J. De Yoreo, X. Lu and K. M. Rosso, *Inorg. Chem.*, 2019, **58**, 16727–16735.